small
NANO MICRO
Hybrid Materials

Synthesis of Silver Nanoparticle–Hollow Titanium Phosphate Sphere Hybrid as a Label for Ultrasensitive Electrochemical Detection of Human Interleukin-6

Juan Peng, Li-Na Feng, Zhong-Jie Ren, Li-Ping Jiang, and Jun-Jie Zhu**

A silver nanoparticle–hollow titanium phosphate sphere (AgNP–TiP) hybrid is successfully synthesized and used as a label for electrochemical detection of human interleukin-6 (IL-6). Hollow TiP spheres with a diameter of 430 nm and an average thickness of 40 nm are synthesized by a template approach. The AgNPs are incorporated in situ into the TiP shell via an exchange process. The as-prepared AgNP–TiP hybrid shows outstanding biocompatibility, good dispersity and solubility in water, and high silver loading properties (289.2 mg of silver in 1.0 g of TiP). These advantages make the AgNP–TiP hybrid an effective candidate as an amplification label in immunoassay systems. Herein, the as-prepared AgNP–TiP hybrid is attached to a signal antibody (Ab_2) to produce Ab_2–AgNP–TiP labels in the fabrication of an electrochemical immunosensor. The nanoparticle-based amplification labels, upon coupling with a magnetic sensing array, give rise to an extremely sensitive response to IL-6 in a linear range of 0.0005–10 ng mL^{-1} with a detection limit of 0.1 pg mL^{-1}. The proposed sensor exhibits high specificity, good reproducibility, and long-term stability, and may be a promising technique for protein and DNA detection.

1. Introduction

The convergence of nanotechnology and biotechnology has led to a great development in the design and fabrication of functional architectures from building blocks such as nanomaterials and biomolecules.[1,2] These assemblies often exhibit unique synergistic properties and are widely used in biosensing,[3] drug and gene delivery,[4] biocatalysis,[5] and other related areas. Nanoparticles, especially metal and semiconductor particles, are widely used as building blocks for these assemblies due to their special electronic, photonic, and catalytic properties.[6,7] Among them, silver nanoparticles (AgNPs) are widely used today in both bioassay and biodiagnostic areas due to their interesting optical and electronic properties.[8,9] When AgNPs are conjugated with biomolecules such as proteins, which have fascinating macromolecular structures in terms of their unique recognition, transport, and catalytic properties, they can act as alternative labels for biological probes,[10] and be useful in electrochemical biosensors or bioassays.[11] However, due to their small size, these AgNP–protein bioconjugates suffer from aggregation, which limits their applications.[12] An alternative and promising strategy is to utilize a biofunctionalized "host" for AgNP loading.

In recent years, there has been a strong interest in hollow spheres because of their wide applications in encapsulation, drug delivery, and so on.[13–16] For most of these applications, the materials used to construct the shells are expected to play an important role in controlling the encapsulation and release kinetics. In some cases, it is also possible to create new features and enable novel applications by using a specific functional material to construct the shells. As an inorganic phosphorus-containing material, titanium phosphate (TiP) was given special attention in the last decade.[17] TiP

J. Peng, L.-N. Feng, Z.-J. Ren, Dr. L.-P. Jiang, Prof. J.-J. Zhu
State Key Laboratory of Analytical Chemistry for Life Science
School of Chemistry and Chemical Engineering
Nanjing University
Nanjing 210093, P. R. China
E-mail: jjzhu@nju.edu.cn; Jianglp@nju.edu.cn

DOI: 10.1002/smll.201101210

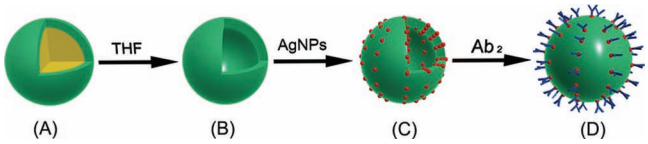

Scheme 1. Schematic illustration of the fabrication process of Ab_2–AgNP–TiP bioconjugates. A) PS@TiP core/shell sphere; B) hollow TiP sphere; C) AgNP–TiP hybrid; D) Ab_2–AgNP–TiP bioconjugate. Ab_2=signal antibody; PS=polystyrene.

has been extensively studied with respect to its potential applications in some areas, such as ion exchange,[18] intercalation,[19] catalysis,[20] and so forth.[21] Layered,[22] nanotube,[23] mesoporous,[24] and nanosphere[20] TiP materials have been successfully synthesized; however, to the best of our knowledge, there is no report on the preparation of hollow TiP spheres. It is believed that TiP with a hollow structure will open up new potential applications, such as drug delivery, bioassay, and biological systems. Therefore, a facile way to prepare TiP hollow spheres is a great challenge and high requirement.

In this work, a silver nanoparticle–hollow titanium phosphate sphere (AgNP–TiP) hybrid was synthesized for the first time and used as a label for electrochemical immunoassay (as illustrated in **Scheme 1**). First, the hollow TiP sphere with a diameter of 430 nm and a shell thickness of 40 nm was synthesized by a template approach. The as-prepared hollow TiP spheres exhibited excellent ion-exchange properties because of their hollow structures and the protons in hydroxyl groups. Then, AgNPs were incorporated in situ into the TiP shell through an ion-exchange process. The hybrid material showed good biocompatibility, outstanding dispersity, and high silver loading properties. The resulting hybrid material could find application in immunoassays.

Human interleukin-6 (IL-6), a pleiotropic cytokine that has a critical role in the inflammatory response, has been implicated in the pathogenesis of a number of inflammatory conditions, such as psoriasis, inflammatory arthritis, cardiovascular disease, and inflammatory bowel disease.[25,26] The normal level in serum is in the range of 10–75 pg mL^{-1}, whereas individuals with various disease states have elevations in IL-6 levels in the ng mL^{-1} range.[27] High levels of IL-6 have also been correlated with prostate cancer of hormone-independent prostate cancer patients,[28] and breast cancer of AIDS patients.[29] Both normal and elevated levels of IL-6 need to be measured accurately for reliable early detection of cancer and disease.

Herein, the signal antibody (Ab_2) was attached to the AgNP–TiP hybrid as a label for the electrochemical detection of human IL- 6. The immunoassay procedure is shown in **Scheme 2**. The immunosensor exhibited a highly sensitive response to human IL- 6. The good result could be ascribed to signal amplification from the large amount of silver loaded into TiP and the reduction of nonspecific adsorption by magnetic separation. This material could be further extended to other bioassay systems and find other applications, such as encapsulation and drug delivery.

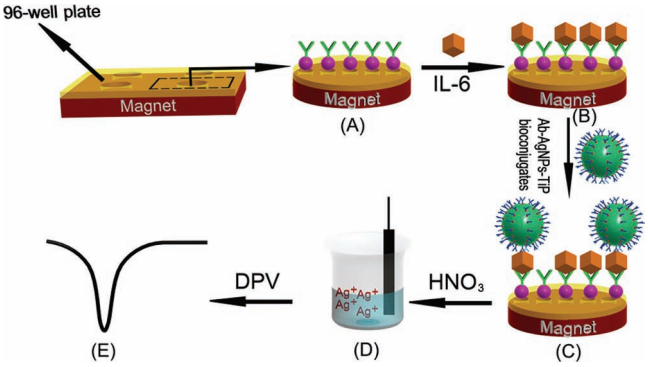

Scheme 2. Schematic illustration of electrochemical immunoassay of IL-6. A) Magnetic sensing array; B) first immunoreaction; C) Ab_2–AgNP–TiP biolabels captured by second immunoreaction; D) release of silver ions by reaction with acid; E) differential pulse voltammetric (DPV) signal of the immunoassay.

2. Results and Discussion

2. 1. Preparation and Characterization of the Hollow TiP Sphere and AgNP–TiP Hybrid

The hollow TiP spheres were synthesized by using PS particles as the templates. $Ti(SO_4)_2$ hydrolyzes easily to TiO_2 precipitates in neutral and basic aqueous solutions. Aqueous $Ti(SO_4)_2$ solution with the addition of 0.1 M H_2SO_4 was stable without the formation of TiO_2 precipitates for at least two months in a sealed vessel. Hydrated titanium chains with different lengths could be formed in an acidic aqueous solution of $Ti(SO_4)_2$.[30,31] The TiP shell was formed through hydrated titanium reaction with phosphate groups from an aqueous phosphate-buffered saline(PBS) solution (**Figure 1**).

Figure 2a and b show typical transmission electron microscopy (TEM) images of the hollow TiP spheres. The as-prepared TiP spheres have a uniform hollow structure with a diameter of about 430 nm and an average shell thickness of about 40 nm. The size of the hollow TiP spheres can be tailored by changing the PS template size.

Layered TiP possesses rich intercalation because the protons in the layers can be exchanged with various kinds of cations.[32,33] The hollow TiP spheres are a similar case to the layered material, and have an abundant amount of hydroxyl groups, which can facilitate the ion-exchange process.[34] AgNPs are incorporated into the TiP shell via the ion-exchange process of silver ions with protons at 50 °C and in situ reduction (as shown in Figure 1). Figure 2c and d display the typical TEM images of the AgNP–TiP hybrid.

It can be clearly observed that a large number of AgNPs with a diameter of about 4–8 nm (**Figure 3**A) are embedded and highly monodispersed in the TiP shell. X-ray photoelectron spectroscopy (XPS) was used to characterize the hollow TiP spheres and the AgNP–TiP hybrid in a wide scan (see Figure 3B). Figure 3B, curve a, shows the spectrum of the hollow TiP spheres. Ti $2p_{1/2}$ and Ti $2p_{3/2}$ peaks are present at binding energies of 465.1 and 459.3 eV, respectively. The signal peak at 133.6 eV corresponds to the peak of P 2p. An

small NANO MICRO

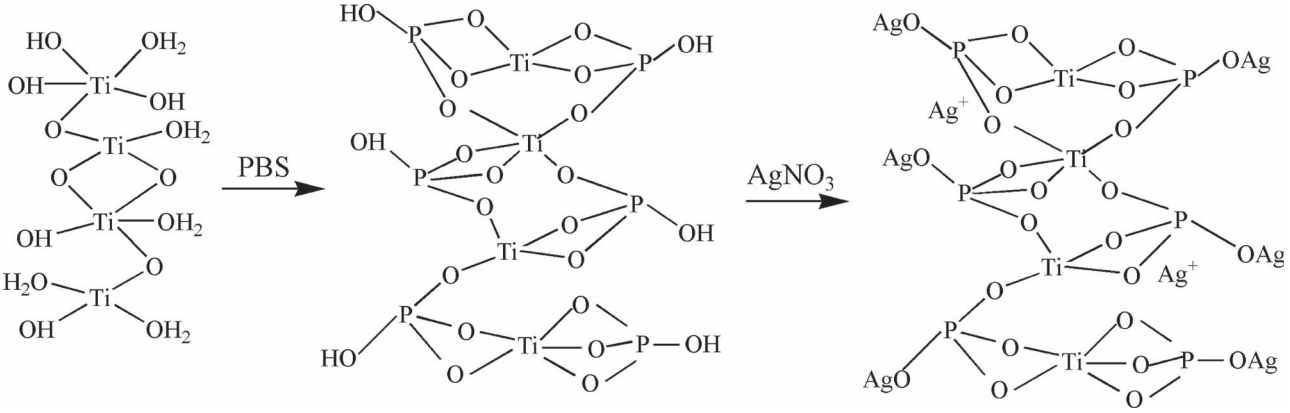

Figure 1. Left: hydrated titanium formed in acidic solution. Middle: TiP formed on PS particles. Right: silver ions exchanged with TiP.

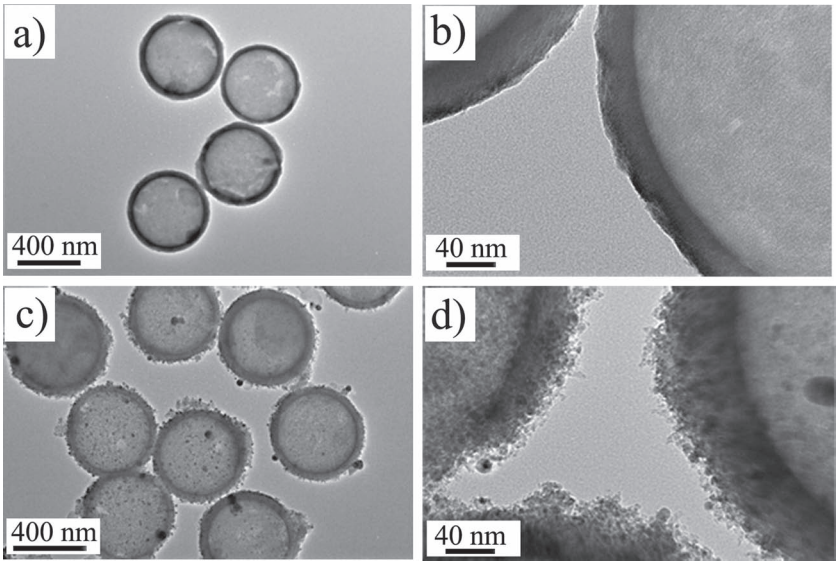

Figure 2. a) Low- and b) high-magnification TEM images of hollow TiP spheres. c) Low- and d) high-magnification TEM images of AgNP–TiP hybrids.

O 1s peak is observed at 531.47 eV, which originates from the O atom in P–O. Compared with the spectrum of pure hollow TiP spheres, new peaks at 368.2 and 374.1 eV emerge in the spectrum of the AgNP–TiP hybrid (Figure 3B, curve b), which correspond to Ag $3d_{5/2}$ and Ag $3d_{3/2}$, respectively, thereby indicating that AgNPs are successfully prepared. UV–vis absorption spectra of the hollow TiP spheres and the AgNP–TiP hybrid spheres are shown in Figure 3C. Compared with the spectrum of the pure hollow TiP spheres (curve a), a new absorption band centered at 444 nm is observed in the spectrum of the AgNP–TiP hybrid (curve b), which is the typical surface plasma resonance band of AgNPs. The result confirmed the formation of AgNPs in the titanium phosphate matrix. Figure 3D shows the powder X-ray diffraction (XRD) pattern of the hollow TiP spheres and the AgNP–TiP hybrid spheres. The as-prepared TiP is amorphous because no diffraction patterns of crystalline titanium phosphate are observed in the XRD spectra (Figure 3D curve a). As shown in Figure 3D curve b, the strong diffraction peaks at the Bragg angles of 38. 7, 44. 2, 64. 5, and 77.4° correspond to the (111), (200), (220), and (311) planes of the AgNPs, respectively. The results confirmed that the AgNPs in the TiP shell were well crystallized. We concluded that the AgNP–TiP hybrid material had been successfully prepared.

The amount of AgNPs intercalated into TiP shells was also measured. The results demonstrate that 289.2 mg of silver is loaded in 1.0 g of TiP. The high loading amount of silver could be ascribed as follows. On the one hand, the hollow structure of TiP provides a promising matrix for the loading of AgNPs inside and outside of the "host". On the other hand, the ion-exchange process offers a simple and efficient way for incorporating silver ions into TiP shells. The hybrid material retains the hollow structure and inherits the advantages of the parent materials, such as good solubility in water, as well as chemical stability. It could potentially be used in bioassay, catalytic, and optical applications.

2. 2. Characterization of Ab_2–AgNP–TiP Bioconjugates

The enormous loading of the AgNPs provides a promising carrier-amplification label for the detection of DNA or protein in clinical diagnosis. To demonstrate its application in immunoassay, the AgNP–TiP hybrid was functionalized with Ab_2.[11] Ab_2 molecules are covalently linked to the AgNP–TiP hybrid by a classical strategy, and could be firmly attached to the silver surface through the interaction between AgNPs and mercapto or primary amine groups of proteins. This process avoided protein crosslinking, and retained their specific immunorecognition ability.[35] The amount of Ab_2 conjugated with the hybrid was determined by monitoring the UV absorption difference at 280 nm. The adsorbed amount of Ab_2 is estimated to be 15.61 μg mL^{-1} in the stock dispersion solution. The FTIR spectrum was used to characterize Ab_2–AgNP–TiP bioconjugates as shown in **Figure 4**.

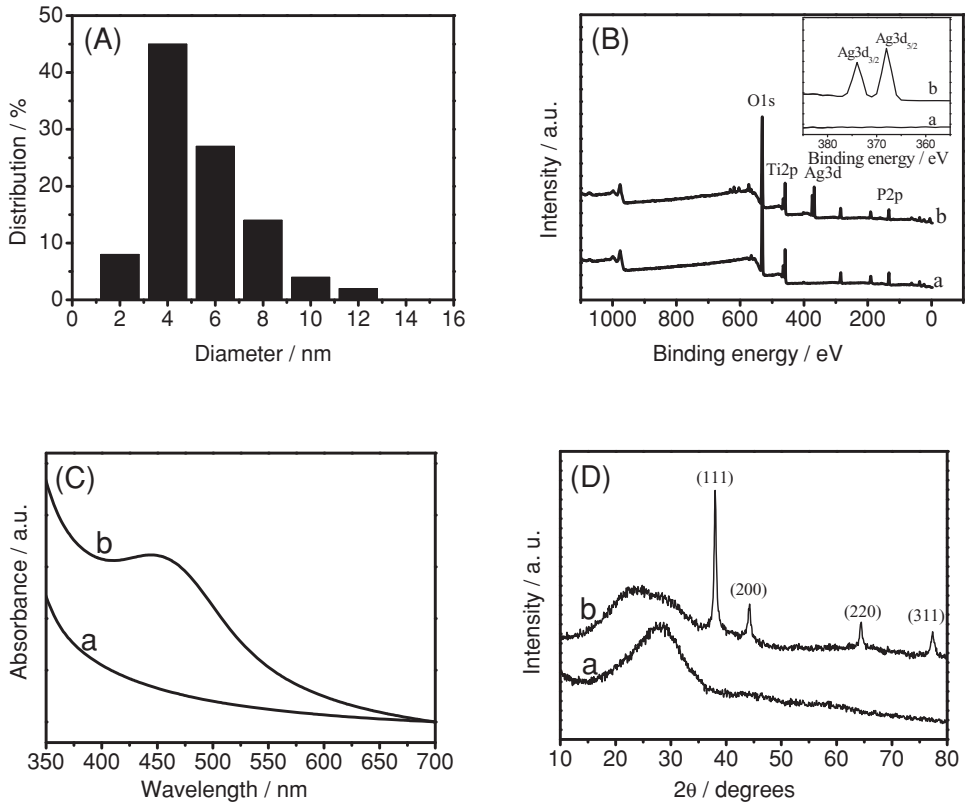

Figure 3. A) Size distribution of AgNPs in the AgNP–TiP hybrid. B) XPS spectrum of a) TiP and b) AgNP–TiP hybrid. C) UV–vis spectrum of a) TiP and b) AgNP–TiP hybrid. D) XRD patterns of a) TiP and b) AgNP–TiP hybrid.

Compared with the spectrum of the AgNP–TiP hybrid (curve a), the transmissions around 1075 and 863 cm^{-1} in curve b match well with that from the amine group of Ab_2.

2. 3. Preparation of a Magnetic Sensing Array for Sandwich Immunoassay

For the fabrication of a magnetic sensing array, capture IL-6 antibody (Ab_1)-functionalized Fe_3O_4 nanoparticles (Fe_3O_4–Ab_1) were assembled on a 96-well microplate via an external magnet. Scheme 2 displays the sandwich immunoassay protocol based on the Ab_2–AgNP–TiP bioconjugates as labels combined with the magnetic sensing array. First, the antigens IL-6 were bound to the Fe_3O_4–Ab_1 via first immunoreaction. Then, the Ab_2–AgNP–TiP bioconjugates were introduced and captured onto the wells by a second immunorecognition event. The captured labels were determined by electrochemical stripping analysis of the silver component after acid dissolution.

2. 4. Stripping Voltammetric Analysis of IL-6

Figure 5 shows typical cyclic voltammograms for the immunoassay. In a control experiment, when the Ab_2–AgNP–TiP

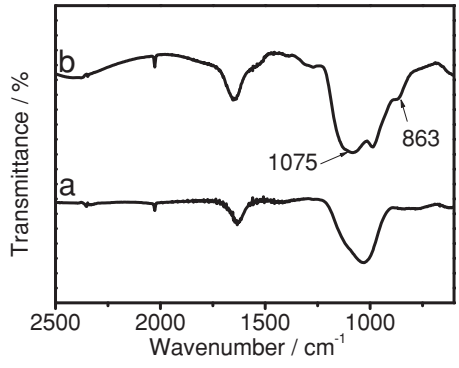

Figure 4. FTIR spectrum of a) AgNP–TiP hybrid and b) Ab_2–AgNP–TiP bioconjugates.

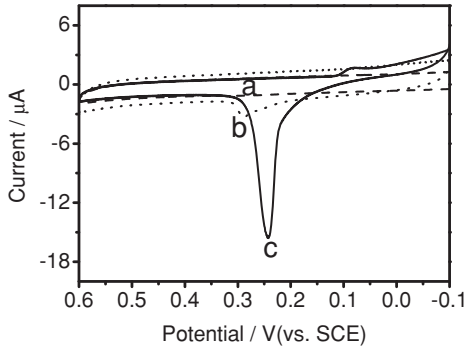

Figure 5. Cyclic voltammograms of electrochemical immunoassay: a) in the absence of IL-6 using Ab_2–AgNP–TiP labels; b) in the presence of 1.0 ng mL^{-1} IL-6 using Ab_2–AgNP labels; c) in the presence of 1.0 ng mL^{-1} IL-6 using Ab_2–AgNP–TiP labels. SCE=saturated calomel electrode.

small NANO MICRO

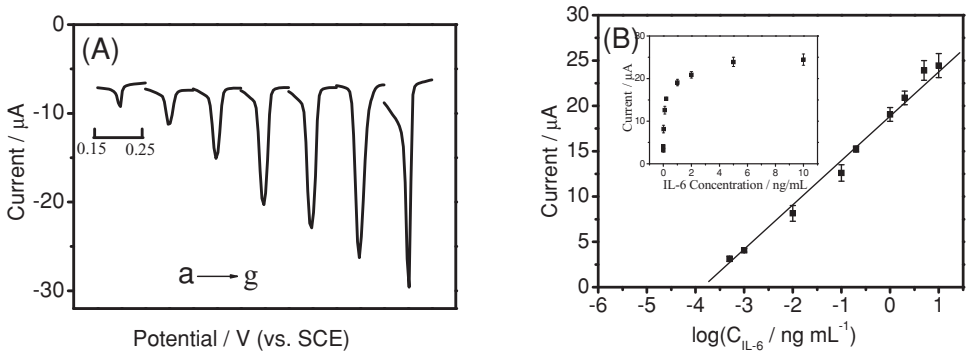

Figure 6. A) Typical DPV curves of electrochemical immunoassay by Ab_2–AgNP–TiP labels with increasing IL-6 concentration from (a) to (g): 0.0005, 0.001, 0.01, 0. 1, 0. 2, 1. 0, and 10 ng mL^{-1} IL- 6, respectively. B) The resulting calibration curve of IL-6 plotted on a semilog scale.

labels were used without exposure to antigen IL- 6, no detectable signals could be observed (curve a). In the presence of IL- 6, a well-defined peak for the oxidation of silver was observed around 0.25 V. The oxidation current of 15.56 μA obtained by using Ab_2–AgNP–TiP labels (Figure 5, curve c) was 5.31 times the current obtained by using Ab_2–AgNP labels (curve b). The result confirmed that the signal was amplified by the Ab_2–AgNP–TiP labels, which could be mainly attributed to the high silver loading on hollow TiP spheres.

The stripping response could be strongly affected by the experimental conditions (see Figure S1 in the Supporting Information). As the deposition potential decreased from –0.1 to –0.8 V, the peak current increased rapidly between –0.1 and –0.5 V and then reached a relative plateau below –0.5 V. As a result, a deposition potential of –0.5 V versus SCE was selected for the study. With the increase of deposition time, the peak current was enhanced and then reached a plateau at about 5 min. Consequently, a deposition time of 5 min was chosen for all of the experiments. The maximum response appeared at a reaction temperature of 37 °C, which could be attributed to denaturing of proteins at higher temperature and low immunoreaction efficiency at lower temperature. The response increased with the incubation time between 10 and 60 min and then leveled off after 40 min. The results indicated that the interaction of antigen with antibody reached equilibrium after 40 min. Therefore, to maximize the signal and minimize the assay time, 40 min was selected as the optimal incubation time. In addition, the response increased with the concentration and reached a plateau at 50 μg mL^{-1} of Ab_2–AgNP–TiP bioconjugates.

Figure 6A displays the typical differential pulse voltammetry (DPV) curves of IL- 6. The peak current increased linearly with the increase of the logarithm of the IL-6 concentration over the range of 0.0005–10 ng mL^{-1}, as shown in Figure 6B. The linear regression equation was $I(\mu A) = 18.87 + 4.890 \log C_{IL\text{-}6}(\text{ng mL}^{-1})$, with a linear regression coefficient of 0.998. The detection limit ($S/N = 3$) was estimated to be 0.1 pg mL^{-1}. The results demonstrated that the proposed methods were highly sensitive, especially for the detection of biomarkers at low levels.

Compared with reported immunoassays (as shown in **Table 1**),[36–40] the proposed assay showed a wider linear range and lower detection limit. The high sensitivity coupled with excellent selectivity could be attributed to the following factors. The excellent ion-exchange property of the hollow TiP sphere promoted a high loading of silver, which provided promising amplification labels. Owing to the good biocompatibility and dispersity, the AgNP–TiP hybrid provided a highly suitable microenvironment for antibody molecules. In addition, the magnetic sensing array offers an ideal and effective platform for the immobilization of Ab_1 and reduces nonspecific adsorption.

Table 1. Analytical properties of other methods for IL-6 immunoassays.

Method	Linear range [ng mL^{-1}]	Detection limit [ng mL^{-1}]	Reference
ELISA	0.039–2.5	0.039	[36]
Fluorescent microarray	0.1–10	0.1	[37]
Conductometric immunosensor	0.03–0.3	0.01	[38]
Fluorescence-based fiber-optic biosensors	0.12–12	0.12	[39]
Amperometric immunosensor	0.004–0.1	0.001	[40]
Magnetic electrochemical immunosensor	0.0005–10	0.0001	this work

Specificity is an important criterion for analytical measurement. Other proteins, such as tumor necrosis factor alpha (TNF-α), human immunoglobulin G (IgG), and carcino-embryonic antigen (CEA), were used to evaluate the selectivity of the immunoassay. The current value obtained for each interfering substance at a concentration of 0.1 ng mL^{-1} was used as an indicator for the assay selectivity in comparison with the IL-6 reading alone. As can be seen in **Figure 7**A, the current values for TNF- α, IgG, and CEA are 4. 1, 5. 2, and 6. 7% that of IL- 6, respectively. This result indicates that the proposed strategy has sufficient selectivity for IL-6 detection, and is capable of differentiating IL-6 from its analogues in complex samples. The immunoassay reproducibility is estimated by assaying one IL-6 level for five replicate measurements (Figure 7B) with a relative standard deviation (RSD) of 6. 0%. The storage stability of the Ab_2–AgNP–TiP was also investigated by comparison with the stripping signals after a sandwich immunoreaction. When the dried Ab_2–AgNP–TiP was stored at 4 °C, the stripping signals

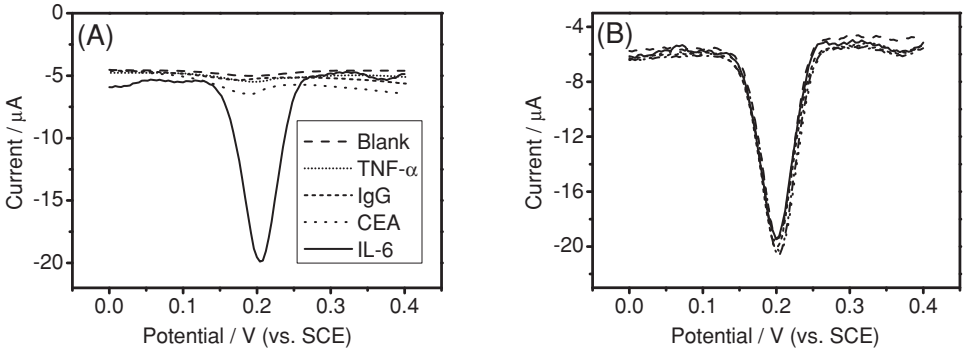

Figure 7. A) DPV curves for the blank and 0.1 ng mL^{-1} TNF- α, IgG, CEA, and IL- 6. B) Five replicate DPV measurements for 0.1 ng mL^{-1} IL- 6.

remained about 94. 2% after two months of storage. This indicates that dried Ab_2–AgNP–TiP has good storage stability at 4 °C. To investigate the variability of the immunoassay system from batch-to-batch fabrication of the hybrid nanoparticles, two different batches of the AgNP–TiP hybrid were used to fabricate the Ab_2–AgNP–TiP labels. The result shows that there is no obvious difference (with RSD of 8. 0%) for the current response when using two batches of labels. This is mainly attributable to the good fabrication reproducibility of the AgNP–TiP hybrid.

The feasibility of the immunoassay for clinical applications was investigated by analyzing real samples, in comparison with the enzyme-linked immunosorbent assay (ELISA) method. To avoid the matrix effect, the response for the serum samples diluted with PBS to different concentrations was investigated. As can be seen in Figure S2 (Supporting Information), there is no obvious effect when the dilution increased to 10 times. **Table 2** presents the correlation between the partial results obtained by the proposed immunoassay and the ELISA method. It obviously indicates that there is no significant difference between the results given by the two methods, that is, the proposed immunoassay could be satisfactorily applied to the clinical determination of IL-6 levels in human plasma.

3. Conclusion

Hollow TiP spheres with highly uniform structure have been successfully synthesized by a template approach. AgNPs were incorporated into a TiP matrix through a simple ion-exchange route. The resulting hybrid could be conjugated with antibody molecules for a bioassay labeling system due to its high water solubility and outstanding biocompatibility. In addition, the enormous loading, coupled with the unique physical and chemical properties of AgNPs, enabled a promising and versatile amplified platform for application in immunoassay. A novel electrochemical immunosensor based on Ab_2–AgNP–TiP labels was constructed to evaluate their feasibility in bioanalytical applications. By combining with a magnetic sensing array, such a hybrid label yields an extremely high sensitivity, a wide linear range of six orders of magnitude, a low detection limit, and a high selectivity for the detection of IL- 6. Due to the interesting structure and unique features, the hollow AgNP–TiP hybrid spheres can also be expected to be used in encapsulation, drug delivery, and so on.

Table 2. Assay results of clinical serum samples using the proposed and ELISA methods.

Serum samples	Proposed method[a)] [pg mL^{-1}]	ELISA[a)] [pg mL^{-1}]	Relative deviation [%]
1	65.52	66.32	–1.2
2	104.4	111.9	–6.7
3	198.1	189.0	4.8
4	98.12	93.26	5.2
5	123.2	121.6	1.3

[a)]The average value of five successive determinations.

4. Experimental Section

Materials and Reagents: Titanium sulfate ($Ti(SO_4)_2$), silver nitrate ($AgNO_3$), sodium borohydride ($NaBH_4$), and tetrahydrofuran (THF) were purchased from Shanghai Chemical Reagent Co. (Shanghai, China). Human interleukin-6 (IL-6), capture (Ab_1) and signal IL-6 antibody (Ab_2) were purchased from Beijing Biosynthesis Biotechnology Co., Ltd. Human serum samples were obtained from the Affiliated Drum Tower Hospital of Nanjing University Medical School, and used as received. Glutaraldehyde, poly(diallyldimethylammonium chloride) (PDDA, MW = 200 000–350 000), bovine serum albumin (BSA), and Tween-20 were from Sigma–Aldrich. Phosphate-buffered saline (PBS) with various pH values was prepared by mixing stock solutions of NaH_2PO_4 and Na_2HPO_4, and then adjusting the pH with 0.1 M NaOH and H_3PO_4. The blocking buffer was 0.01 M, pH 7.4 PBS containing 1 wt% BSA. The wash buffer (PBST) was 0.01 M, pH 7.4 PBS containing 0.05% Tween-20. Other reagents were of analytical grade. Ultrapure fresh water obtained from a Millipore water purification system (MilliQ, specific resistivity larger than 18 MΩ m, Millipore S. A., Molsheim, France) was used in all runs.

Preparation of Hollow TiP Spheres: Monodispersed polystyrene (PS) particles about 500 nm in size were prepared according to our previous report.[41] First, the PS particles were dispersed in PDDA aqueous solution (5 mg mL^{-1} in 0.5 M NaCl) and ultrasonicated for 20 min. The positively charged PS particles were immersed in an aqueous solution of 10 mM $Ti(SO_4)_2$ in 0.1 M H_2SO_4 and sonicated for 10 min. Then, the particles were immersed in PBS (pH 4. 0) and

small NANO MICRO

sonicated for 10 min. Finally, the hollow TiP spheres were prepared by dissolving PS cores in THF for 24 h.

In Situ Preparation of AgNP–TiP Hybrid: First, the as-prepared hollow TiP spheres were immersed in 10 mM $AgNO_3$ aqueous solution at 50 °C for 24 h. Then, the particles were rinsed with water and immersed in freshly prepared 10 mM $NaBH_4$ aqueous solution and stirred for 10 min. After rinsing with water, the AgNP–TiP hybrid was obtained and dispersed in 50 mM Tris–HNO_3 (pH 8. 9) solution.

Preparation of Ab_2–AgNP–TiP Bioconjugates: At room temperature, Ab_2 (1.0 mg mL^{-1}, 200 μL) was added to AgNP–TiP hybrid dispersed in Tris–HNO_3 solution (4.0 mL, pH 8. 9). Then, the mixture was shaken overnight. The mixture was centrifuged and washed with buffer and dispersed in PBST (4.0 mL) that contained 1% BSA.

Preparation of Magnetic Sensing Array: The Fe_3O_4–Ab_1 conjugates were prepared by a modified protocol according to reference [42]. In the immunoassay, the Fe_3O_4–Ab_1 suspension was diluted with the PBST solution. For fabrication of the magnetic sensing array, a 96-well microplate was washed with nitric acid solution, acetone, and doubly distilled water, and dried at room temperature. Then, the 96-well microplate was immobilized on an external magnet. After that, Fe_3O_4–Ab_1 suspension (1.0 mg mL^{-1}, 25 μL) was added to the wells and the following immunoassay was performed.

Immunoassay: First, different concentrations of IL-6 antigen (25 μL) were added to the wells and reacted for 40 min at 37 °C. After washing, Ab_2–AgNP–TiP bioconjugates (25 μL) were added and incubated at 37 °C for 40 min to form a sandwich complex. After washing, HNO_3 (0.1 M, 100 μL) was added to release silver ions from the complex. The suspension containing the released silver ions was transferred to the electrochemical cell for stripping. DPV analysis was conducted using a CHI660 electrochemical workstation equipped with a stirring machine. The electrochemical procedure involved a pretreatment at +0.2 V for 1 min, electrodeposition at –0.5 V for 5 min, and stripping from 0 to 0.5 V using differential pulse voltammetry: 0.05 V amplitude, 4 mV increment, 0.05 S pulse width.

Apparatus: TEM images were obtained on a JEOL JEM-200CX transmission electron microscope with an accelerating voltage of 200 kV. XPS measurements were carried out with an ESCALAB MK II X-ray photoelectron spectrometer. XRD patterns were obtained with a Philips X'Pert X-ray diffractometer with a $Cu_{K\alpha}$ X-ray source. UV–vis absorption spectra were recorded on a UV-2401PC spectrometer. Fourier transform infrared (FTIR) spectroscopic measurements were obtained on a Bruker model Vector22 Fourier transform spectrometer using KBr pressed disks. Inductively couple plasma–atomic emission spectroscopy (ICP-AES, J-A1100, Jarrell-Ash, USA) was used to detect the quantity of silver in the AgNP–TiP hybrid. Electrochemical experiments were performed with a CHI660 workstation (Shanghai Chenhua, Shanghai, China) by using a conventional three-electrode system with a modified glassy carbon electrode (GCE) as working electrode, a saturated calomel electrode (SCE) as reference, and a platinum wire as counter electrode.

Supporting Information

Supporting Information is available from the Wiley Online Library or from the author.

Acknowledgements

We greatly appreciate the support of the National Natural Science Foundation of China (20821063, 21075061, 21020102038). This work was also supported by the National Basic Research Program of China (2011CB933502). The authors thank Prof. Kui Zhang from Nanjing Drum Tower Hospital for her kind help.

[1] R. W. Murray, *Chem. Rev.* **2008**, *108*, 2688.
[2] S. N. Kim, J. F. Rusling, F. Papadimitrakopoulos, *Adv. Mater.* **2007**, *19*, 3214.
[3] J. Wang, *Small* **2005**, *1*, 1036.
[4] V. Salgueirino-Maceira, M. A. Correa-Duarte, *Adv. Mater.* **2007**, *19*, 4131.
[5] J. Lee, Y. Lee, J. K. Youn, H. B. Na, T. Yu, H. Kim, S. M. Lee, Y. M. Koo, J. H. Kwak, H. G. Park, H. N. Chang, M. Hwang, J. G. Park, J. Kim, T. Hyeon, *Small* **2008**, *4*, 143.
[6] M. De, P. S. Ghosh, V. M. Rotello, *Adv. Mater.* **2008**, *20*, 4225.
[7] R. Gill, R. Polsky, I. Willner, *Small* **2006**, *2*, 1037.
[8] P. Rijiravanich, M. Somasundrum, W. Surareungchai, *Anal. Chem.* **2008**, *80*, 3904.
[9] J. Y. Kim, J. S. Lee, *Chem. Mater.* **2010**, *22*, 6684.
[10] S. Kittler, C. Greulich, J. S. Gebauer, J. Diendorf, L. Treuel, L. Ruiz, J. M. Gonzalez-Calbet, M. Vallet-Regi, R. Zellner, M. Koller, M. Epple, *J. Mater. Chem.* **2010**, *20*, 512.
[11] J. Ling, Y. F. Li, C. Z. Huang, *Anal. Chem.* **2009**, *81*, 1707.
[12] H. Li, Z. Y. Sun, W. Y. Zhong, N. Hao, D. K. Xu, H. Y. Chen, *Anal. Chem.* **2010**, *82*, 5477.
[13] J. Yang, J. Lee, J. Kang, K. Lee, J. S. Suh, H. G. Yoon, Y. M. Huh, S. Haam, *Langmuir* **2008**, *24*, 3417.
[14] S. H. Lee, H. E. Jeong, M. C. Park, J. Y. Hur, H. S. Cho, S. H. Park, K. Y. Suh, *Adv. Mater.* **2008**, *20*, 788.
[15] Y. Zhao, L. Jiang, *Adv. Mater.* **2009**, *21*, 3621.
[16] X. W. Lou, C. M. Li, L. A. Archer, *Adv. Mater.* **2009**, *21*, 2536.
[17] A. Clearfield, D. S. Thakur, *Appl. Catal.* **1986**, *26*, 1.
[18] K. M. Parida, B. B. Sahu, D. P. Das, *J. Colloid Interface Sci.* **2004**, *270*, 436.
[19] S. Patoux, C. Masquelier, *Chem. Mater.* **2002**, *14*, 5057.
[20] J. H. Liu, X. F. Wei, Y. L. Yu, J. L. Song, X. Wang, A. Li, X. W. Liu, W. Q. Deng, *Chem. Commun.* **2010**, *46*, 1670.
[21] H. Takahashi, T. Oi, M. Hosoe, *J. Mater. Chem.* **2002**, *12*, 2513.
[22] P. Curnow, P. H. Bessette, D. Kisailus, M. M. Murr, P. S. Daugherty, D. E. Morse, *J. Am. Chem. Soc.* **2005**, *127*, 15749.
[23] Z. L. Yin, Y. Sakamoto, J. H. Yu, S. X. Sun, O. Terasaki, R. R. Xu, *J. Am. Chem. Soc.* **2004**, *126*, 8882.
[24] C. L. Pan, W. X. Zhang, Y. L. Wang, Z. Zhou, D. Z. Jiang, S. J. Wu, T. H. Wu, *Mater. Lett.* **2003**, *57*, 3815.
[25] G. A. Messina, N. V. Panini, N. A. Martinez, J. Raba, *Anal. Biochem.* **2008**, *380*, 262.
[26] W. E. Naugler, M. Karin, *Trends Mol. Med.* **2008**, *14*, 109.
[27] K. Z. Liang, J. S. Qi, W. J. Mu, Z. X. Liu, *Bioproc. Biosyst. Eng.* **2009**, *32*, 353.
[28] L. T. May, H. Viguet, J. S. Kenney, N. Ida, A. C. Allison, P. B. Sehgal, *J. Biol. Chem.* **1992**, *267*, 19698.
[29] J. Domingo-Domenech, C. Oliva, A. Rovira, J. Codony-Servat, M. Bosch, X. Filella, C. Montagut, M. Tapia, C. Campas, L. Dang, M. Rolfe, J. S. Ross, P. Gascon, J. Albanell, B. Mellado, *Clin. Cancer Res.* **2006**, *12*, 5578.
[30] T. P. Niesen, J. Bill, F. Aldinger, *Chem. Mater.* **2001**, *13*, 1552.
[31] Q. F. Wang, L. Zhong, J. Q. Sun, J. C. Shen, *Chem. Mater.* **2005**, *17*, 3563.
[32] A. Clearfield, *Chem. Rev.* **1988**, *88*, 125.

[33] G. Cao, L. K. Rabenberg, C. M. Nunn, T. E. Mallouk, *Chem. Mater.* **1991**, *3*, 149.
[34] Q. F. Wang, H. J. Yu, L. Zhong, J. Q. Liu, J. Q. Sun, J. C. Shen, *Chem. Mater.* **2006**, *18*, 1988.
[35] R. J. Cui, H. P. Huang, Z. Z. Yin, D. Gao, J. J. Zhu, *Biosens. Bioelectron.* **2008**, *23*, 1666.
[36] C. K. Turner, T. M. Blieden, T. J. Smith, S. E. Feldon, D. C. Foster, P. J. Sime, R. P. Phipps, *J. Immunol. Methods* **2004**, *291*, 63.
[37] H. Wu, Q. S. Huo, S. Varnum, J. Wang, G. G. Liu, Z. M. Nie, J. Liu, Y. H. Lin, *Analyst* **2008**, *133*, 1550.
[38] K. Z. Liang, W. J. Mu, M. Y. Huang, Z. X. Yu, Q. K. Lai, *Electroanalysis* **2006**, *18*, 1505.
[39] R. Kapoor, C. W. Wang, *Biosens. Bioelectron.* **2009**, *24*, 2696.
[40] G. F. Wang, H. Huang, G. Zhang, X. J. Zhang, B. Fang, L. Wang, *Langmuir* **2011**, *27*, 1224.
[41] X. M. Feng, C. J. Mao, G. Yang, W. H. Hou, J. J. Zhu, *Langmuir* **2006**, *22*, 4384.
[42] H. Wang, J. Wang, C. Timchalk, Y. H. Lin, *Anal. Chem.* **2008**, *80*, 8477.

Received: June 17, 2011
Revised: July 11, 2011
Published online: August 23, 2011

